Solar Physics
DOI: 10.1007/•••••-•••-•••-••••-•

The Ulysses catalog of solar hard X-ray flares

C. Tranquille[1] · **K. Hurley**[2] · **H. S. Hudson**[2]

Abstract *Ulysses* was launched in October 1990, and its Solar X-ray/Cosmic Gamma-ray Burst Experiment (GRB) has provided more than 13 years of uninterrupted observations of solar X-ray flare activity. Due to the large variation of the relative solar latitude and longitude of the spacecraft orbit with respect to the Earth, the perspective of the GRB instrument often differed significantly from that of X-ray instruments on Earth-orbiting satellites. During extended periods the GRB made direct observations of flares on the hidden face of the Sun, providing a unique record of events not visible to other instruments. The small area of GRB and its optimization for very high counting rates minimized the effects of pulse pile-up. We interpret the spectra, time histories, and occurrence distribution patterns of GRB data in terms of "thermal feedthrough," the confusion of thermal soft X-rays and non-thermal hard X-rays. This effect is a systematic problem for scintillation-counter spectrometers observing the solar hard X-ray spectrum.

This paper provides a definitive catalog of the *Ulysses* X-ray flare observations and discusses various features of this unique data base. For the equivalent GOES range X2-X25, we find a power-law fit for the (differential) occurrence frequency at >25 keV with slope -1.61±0.04, with no evidence for a downturn at the highest event magnitudes.

1. Introduction

Solar hard X-rays result from the interaction of energetic electrons with ions present in the ambient solar atmosphere (e.g., Dennis, 1985; Hudson and Ryan, 1995). Electrons, accelerated to energies above ∼20 keV by processes not yet properly understood, emit continuum hard X-radiation predominantly at the chromospheric footpoints of coronal magnetic loops. Softer X-rays have thermal spectra with kT = 1-3 keV and originate from the loops themselves. The soft X-ray emission lags in time according to the Neupert effect (Neupert, 1968; Dennis and Zarro, 1993). The duration of the hard X-ray emissions can vary from a

[1] Research and Scientific Support Department, ESA/ESTEC, Postbuss 299, 2200 AG Noordwijk, The Netherlands email: Cecil.Tranquille@esa.int
[2] Space Sciences Lab, UC Berkeley

few seconds to many tens of minutes and the photon energies can extend to the highest limit of the observations.

One of the scientific objectives of the GRB experiment flown on *Ulysses* (Hurley *et al.*, 1992) was to make stereoscopic observations of solar flares from its unique high-latitude heliocentric orbit by comparison with data from other X-ray monitors flown on satellites in near-Earth or other interplanetary orbits (Hurley, 1986). Combining simultaneous measurements of solar X-rays from two or more satellites having different vantage points can provide useful information about the directivity of the emission as well as an estimate of the height of the emitting region in the photosphere. Deep-space observations contribute to the detection of flares occulted by the solar limb, a good method for isolating X-ray sources in the corona rather than at the chromospheric footpoints of the flare loop system (Frost and Dennis, 1971; Hudson, 1978; Kane *et al.*, 1998).

The large aphelion distance of the *Ulysses* orbit ($\sim$5 AU), as well as the small size of the GRB detectors, helped to minimize saturation during the most energetic events. Detectors flown on spacecraft in orbits closer to the Sun can suffer from saturation and pulse pile-up effects at these times, resulting in reduced fidelity of the time profiles, especially around event maxima. This orbit also permitted almost continuous observations, as opposed to the regular eclipses due to Earth occultation in low Earth orbit, the usual site for solar hard X-ray observations.

Ulysses, although still functional, no longer routinely returns the basic data stream from GRB most suitable for solar hard X-ray observations. This is therefore an appropriate time to present the catalog of its observations, and that is the main function of this paper. We identify 59 GOES X-class flares observed simultaneously by GRB, and separately list another 14 comparable events for which the solar source was occulted by the solar disk as seen by *Ulysses*. The catalog of GRB information on these events is presented in tabular form in this paper, and also on-line as text and image files of the time histories. For the most energetic events there is substantial concern about pulse pileup (as with many solar hard X-ray detectors; see Kane and Hudson (1970) and Kane *et al.* (1980)). Accordingly we have carried out a detailed comparison with RHESSI observations of a GOES X8.3 flare, as reported in Appendix A. We also describe Monte Carlo simulations of pulse pileup in the GRB instrument in Appendix B; in general this is not as important an effect for GRB as it has been for other instruments for the reasons (great distance, small area) given above.

2. The GRB Instrument

The Gamma-Ray Burst (GRB) instrument, has been described in detail elsewhere (Hurley *et al.*, 1992). The two hard X-ray detectors are hemispherical shells of CsI(Tl) scintillators, with thickness 3 mm and diameter 51 mm, coupled by plastic light-guides to photomultiplier tubes. The detectors are mounted externally on a $\sim$3 m boom. This remote mounting gives essentially all-sky coverage and also reduces the contamination from the radioactive source used

by the spacecraft as a source of power throughout the mission (a radioisotope thermoelectric generator, or RTG). The two detectors together provide an approximately isotropic response, with a projected area of about 20 cm^2 in all directions. They were continuously calibrated with a ^{241}Am source; energy spectra were read out on a daily basis to track the position and resolution of the ∼60 keV line from this radioisotope. The day-to-day gain variations proved to be negligible, and the longer-term variations were compensated by analysis software and by adjusting the high voltage to the photomultiplier tubes. We were fortunate that *Ulysses* overlapped with RHESSI, and we have used a flare that was well observed by both instruments for a check on this calibration and other potential problems (Appendix A). The detector outputs are summed on board the spacecraft, and provide the integral counting rate over the spectral range 25-150 keV with a time resolution of 0.25-2 s, depending on the telemetry rate of the downlink. The background counting rate of the GRB instrument in this band is typically about 500 counts s^{-1}; for solar observations this corresponds to ∼25 ph $(cm^2 s)^{-1}$ above 25 keV. A soft X-ray (5-20 keV) detector comprising two Si sensors also formed part of the GRB instrument, but it became noisy during the unexpectedly long waiting period prior to launch and did not produce useful results. Spectral information in the hard X-ray range is available when the instrument automatically triggers into "burst mode" following a rapid increase in the detector count rate due to a cosmic gamma-ray burst or a solar flare, but we do not make use of this data mode for the catalog described in this paper. The instrument began observations in October 1990, and with the exception of a few periods, such as the Jupiter encounter in February 1992, it remained in continuous operation until November 2003. At this time, the RTG power became insufficient to keep all the experiments on. Prior to this, the data recovery from the mission was over 95%, and the GRB experiment observed over 1500 solar flare X-ray events (a list may be found at http://helio.esa.int/ulysses/ftp/public/outgoing/ and in the on-line material for this paper).

For the biggest events the GRB data require corrections for dead time and for counter rollover. We base the dead-time corrections on pre-launch calibrations. Figure 1 shows an example of the large X-ray event observed by GRB on June 1, 1991, that required correction for both rollover and dead time effects. The nominal energy resolution of GRB is 40% at 60 keV, reflecting its optimization for high counting rates rather than high resolution.

3. Thermal vs. nonthermal hard X-rays

Solar hard X-ray spectroscopy presents particular observational problems because of the great dynamic range in source brightness. One of the most worrisome of these is pulse pile-up (Kane and Hudson, 1970; Datlowe, 1975), which we deal with in Appendix B. Inorganic scintillators such as the CsI(Tl) of *Ulysses*, or the CsI(Na) of SMM (Orwig, Frost, and Dennis, 1980), have good photopeak efficiencies but also relatively slow pulses, which exacerbates this problem.

In addition to this difficulty there is the problem of the intense soft X-ray spectrum. A solar flare may have a very large spectral intensity at a few keV,

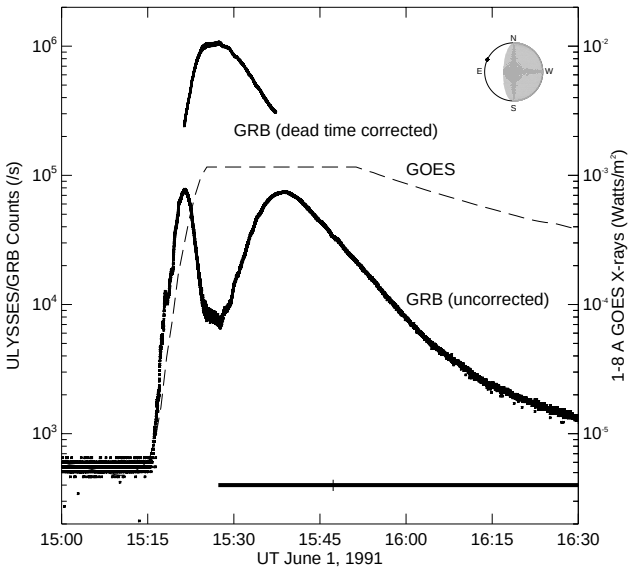

Figure 1. A solar flare measured by *Ulysses* GRB (June 1, 1991, day 152; see Kane *et al.*, 1995). The raw GRB count rate recorded by the instrument (after correction for buffer overflow) is plotted in the lower curve, with the deep minimum seen in the time profile due to dead time. The upper points show the true count rate with full corrections. The dashed line shows the GOES low channel, which saturates for an event of this magnitude. The GOES times are corrected for light travel time to the position of *Ulysses*. The inset of the solar disk shows the view of the Sun from Earth, shaded for regions not visible from the position of *Ulysses*. The location of the flare is marked by an asterisk.

in a spectrum with a steep exponential falloff (kt $\sim$3 keV) to higher energies. Because scintillation counters have relatively poor energy resolution, pulses from this component can readily be confused with those from true hard X-rays. This "thermal feed-through" effect can be seen in most solar hard X-ray photometers, especially those with relatively thin entrance windows. It is systematically more important for flares of greater magnitude because of the general correlation of soft X-ray effective temperature with emission measure (Garcia and McIntosh, 1992; Feldman, 1996). For this reason events such as that of Figure 1 tend to show smooth "hard X-ray" light curves, which for a fixed threshold show relatively more thermal component. Note that this is independent of considerations of pulse pile-up effects and only depends upon the relative magnitudes of the thermal and non-thermal components.

High-resolution observations with Ge detectors (Lin *et al.*, 1981), now carried out systematically with the Reuven Ramaty High-Energy Solar Spectrometric Imager spacecraft (RHESSI) (e.g. Holman *et al.*, 2003), make it clear that this artifact complicates all solar hard X-ray catalogs derived from scintillation counters. Interestingly, it also makes it very difficult to recognize the analogous

thermal/nonthermal components of stellar hard X-ray spectra because of their still higher thermal temperatures (Osten *et al.*, 2007).

4. Observations

4.1. GOES events

Information relevant to this study was extracted from the NOAA reports for all of the X-class flares recorded by GOES since the launch of *Ulysses* in October 1990 until the GRB instrument was temporarily switched off in November 2003. Table 1 lists the 159 X-class flare events used in this report from the NOAA catalogs. The GRB rates are scaled to 1 AU. The date of each event is provided, together with its start and end times (at GOES), and the time of the peak seen in the GOES X-ray time profile. In addition, the flare location (solar longitude and latitude) and peak flux are given. From the position of the *Ulysses* spacecraft (radial distance, solar longitude and latitude, also tabulated), we calculate whether the GOES flare should have been visible or not from the viewpoint of *Ulysses*. This is done by determining the angle (also given in Table 1) between the position of *Ulysses*, the center of the Sun, and the location of the flare on the solar surface. If this angle is between 0° and 90°, then the flare is on the hemisphere of the Sun visible to *Ulysses*. An angle of 180° represents a point on the hidden hemisphere of the Sun, directly opposite to the position of *Ulysses*. For 18 events, the location of the flare on the solar surface is not known from the NOAA reports, so it is not possible to determine unambiguously whether they could be seen by GRB or not.

Figure 2 displays the locations of the X-class flares on the visible hemisphere of the Sun (as seen from Earth) using the data from the SGAS reports. As is well known (Smith and Smith, 1963), flares cluster around mid-latitude bands north and south of the solar equator. There can also be significant asymmetry in the number of flares seen in the two hemispheres as discussed, e.g., in (Garcia, 1990).

A significant concurrent increase in the GRB count rate (Y/N in Table 1) was required to confirm that each GOES X-class event calculated to be visible from the position of *Ulysses*, was indeed seen. Of the 65 events seen by GOES that should also have been detected by *Ulysses*, 59 events registered a count rate increase in the GRB instrument as expected. A single event (May 29, 1991, GOES class X1) showed no signature in the count rate profile, possibly due to the combination of a steep hard X-ray spectrum and the relatively large radial distance (3.17 AU) of *Ulysses*. A further three events showed no apparent signature in the GRB data due to a high instrument background resulting from contamination by *in situ* solar protons. Two events could not be verified at all because of data gaps in the GRB telemetry. Thus the *Ulysses* GRB data are consistent with the hypothesis that an X-class flare always has a hard, non-thermal emission component, which in most cases extends well above 25 keV.

In addition to the flares predicted to be visible from the orbit of *Ulysses*, there were another 14 flares which were recorded by GRB from behind the solar limb.

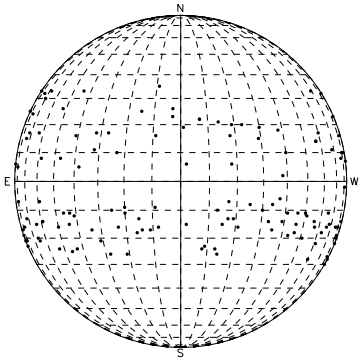

Figure 2. Heliographic locations of all X-class flares observed by GOES over the GRB observing interval (October 1990 to late 2003).

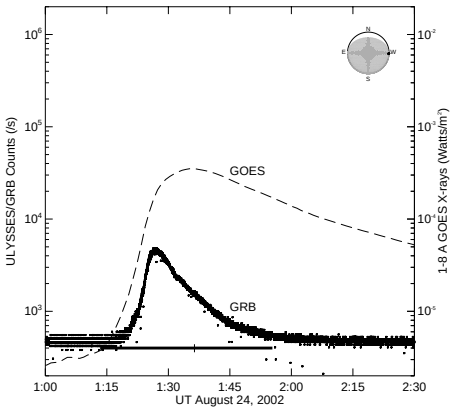

Figure 3. An example of an X-class flare measured by GOES that was behind the solar limb as viewed from the orbit of Ulysses. The hemisphere shown is that seen from the Earth. The unshaded region shows is the part of this hemisphere which Ulysses was able to see at the time of the flare (August 24, 2002), when the spacecraft was at heliographic coordinates (179.5W, 41.2N). The flare was located on the hidden hemisphere of the Sun as viewed from Ulysses, but was sufficiently close to the solar limb to register X-ray photons in the GRB detector.

The *Ulysses*-Sun-flare angle for these events ranged from 90° to no more than 110°. Figure 3 is an example of such a flare, showing the relative location of the flare site to the solar limb. Note that the N or S limb may be involved in the flare occultation as viewed from *Ulysses*, rather than the predominant E or W limb as viewed from the Earth. Figures showing the GRB responses to the 63 flares directly visible to GRB and the 14 flares occurring behind the limb (as seen from *Ulysses*,) may be found at http://helio.esa.int/ulysses/ftp/public/outgoing/ and in the on-line material for this paper.

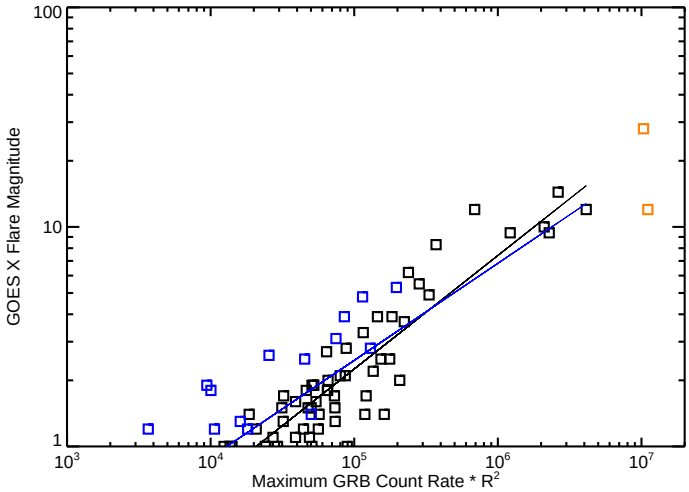

Figure 4. X-class flares seen by both GOES and GRB are used to establish the scaling law between the normalized maximum count rate registered by GRB and the intensity assigned to the flare from GOES measurements. The 59 flares fully visible to both GOES and GRB were used to obtain the fit (black boxes), excluding the two most intense flares measured by GRB (red boxes), one of which was the X28 event of November 4, 2003, and the other the event of June 1, 1991 shown in Figure 1. The 14 flares seen from behind the solar limb from the viewpoint of Ulysses are also plotted (blue boxes), although they are not used in the fit.

4.2. Scaling law

The 59 common events seen by both GOES and GRB were analyzed to establish a correlation between the intensity assigned to the flares in the SGAS reports, and the maximum GRB count rate after normalization for the radial distance of Ulysses. Excluding the data points for the two largest events (red boxes) seen by GRB (the event shown in Figure 1 and the X28 event of November 4, 2003), we find a power-law fit through the common events measured (black boxes) by both GOES (peak energy flux F_{GOES}, 10^{-4} Watts m^{-2}, or X1 units) and GRB (peak count-rate excess F_{GRB}, counts s^{-1}), as shown in Figure 4;

$$F_{GOES} = a(F_{GRB})^b$$

and we find $a = 0.013 \pm 0.003$ and $b = 0.47 \pm 0.02$. This fit also excludes data for the 14 behind-the-disk events because of the bias due to partial occultation of the GRB source. Indeed, these events lie well to the left (thus a lower normalized GRB count rate) of events with similar GOES flare classification seen directly on the hemisphere visible to Ulysses. The derived scaling law is significantly non-linear. This could be the result of systematic error in either (or both) of the data sets, or it could reflect the presence of new mechanisms found in X-class flares but not in less energetic ones. The non-linearity does not reflect selection bias, since selection via the GOES data has given us a complete sample.

This scaling law deviates from the rough proportionality expected from other observations, in particular the slope 0.83 found by Battaglia, Grigis, and Benz

(2005) for a comparison of GOES with the RHESSI 35 keV spectral flux. We believe RHESSI to be the most definitive because its spectral resolution permits it to isolate the non-thermal component more cleanly than previous instruments based on scintillation counters. Our correlation result, b $\sim$ 0.5, differs strikingly from the RHESSI result. We interpret this as evidence for systematic thermal feedthrough into the >25 keV GRB counting rates. The departure from proportionality is in the sense expected from the weak statistical correlation found between GOES temperature and emission measure, as discussed in Section 3. In Appendix A, the GRB thermal feedthrough is shown to be about a factor of 2 for an X8.3 flare. Assuming exact proportionality and fitting only to the events below GOES X10, we find F_{GOES} = A F_{GRB}, with A = (3.0$\pm$0.5) X1 units per GRB count s^{-1}.

4.3. The most energetic events

During the last (Cycle 22) and the present (23) solar cycles, *Ulysses*/GRB successfully recorded the most energetic solar flares (Kane *et al.*, 1995), among which the major flare of November 4, 2003, was the most notable (Kane, McTiernan, and Hurley, 2005). Kane, McTiernan, and Hurley (2005) and others have used the term "giant flare" to describe these top few flares, typically at GOES level X10 or above; they speculated that such flares utilize the bulk of the magnetically stored energy. We do not now regard a "giant flare" as a physically distinct category and believe that many of the reported properties of these events result from the thermal feedthrough mechanism described in Section 3 and in Appendix A. These events saturate GOES and we have used the GRB response as a check on the effective GOES classification of the November 4, 2003 event, one of the most energetic flares on record. An extrapolation of the GOES X-ray count rates during the 15 min of detector saturation was consistent with a flare classification greater than X28 (Kiplinger and Garcia, 2004). Separate studies using the phase of VLF radio signals propagated in the ionosphere (Thomson, Rodger, and Dowden, 2004), and the measurement of the ionospheric attenuation of the galactic radio background (Brodrick, Tingay, and Wieringa, 2005), yielded higher estimates of the peak flux, as high as X40.

We use the scaling law derived in the previous section to estimate a flare class of X24.8$\pm$1.4 from the normalized peak count rate recorded by GRB at 20:34 UT on November 4, 2003 (Figure 5); this uncertainty is only formal since it is probably better than the photometric calibration of GRB, which we estimate at 10-20% (see Appendix A). This result is consistent with the value obtained by a smooth extrapolation of the GOES data when the X-ray sensor saturated. From GRB measurements, the November 4, 2003 flare was slightly exceeded by the flare on June 1, 1991 (Figure 1), which was located at latitude 25°N and probably about 15° behind the east limb in active region 6659. This flare was only classified as an X12 event by GOES, but it is quite likely that this was a much larger event which was significantly underestimated due to its probable occultation by the solar limb as viewed from Earth. According to the study of Tomczak (2001) the depth of occultation in this case was great enough to obscure the footpoint regions of the flare. Because the GRB flux exceeded that expected

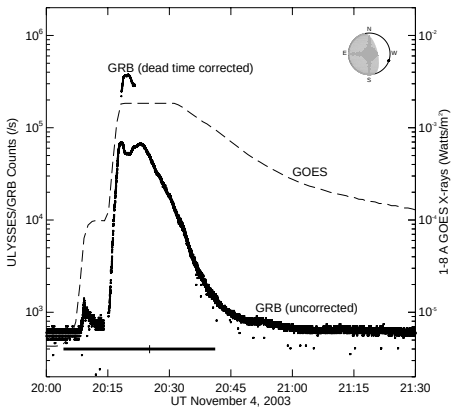

Figure 5. The response of the GRB instrument during the X28 flare on November 4, 2003. The large radial distance of *Ulysses* from the Sun allowed this flare to be monitored throughout its duration without significant saturation of the X-ray photon detectors..

from the correlation, we suggest retrospectively that this flare also belongs in the same category, with effective GOES class above X20. Such large events are few in number and at the limit of our scaling law, so this conclusion is speculative, but we note the event of March 30, 1969 (Frost and Dennis, 1971, also deeply disk-occulted) as another possible example.

4.4. Occurrence distribution function

The GRB observations provide the most extensive and homogeneous view of solar hard X-ray events to date, comparable in length to that of the Solar Maximum Mission (Dennis, 1988), but with a better duty cycle and a dynamic range that favors (because of small detector area and distant orbit) the most energetic events. As noted by Hudson (1991), the distribution function of flare energies follows such a flat power law that it would diverge at large energies, so that an upper limit or at least a roll-over of the distribution is necessary. The GRB database gives us an opportunity to define the occurrence frequency of the most energetic events (i.e., out to the two major flares discussed above) and to investigate whether the distribution follows the expected flat power law.

Figure 6 shows the integral distribution for the 59 well-observed events of Table 1 with accompanying GOES events. We fit this with a simple power-law and find no evidence for a cutoff. On the basis of the number of events in our complete sample, it would be necessary to observe for several solar cycles to improve on this conclusion, or else to use proxy data that contain a longer historical record (e.g., Reedy and Marti, 1991). There is good evidence from cosmic-ray proxies for a steepening of the distribution of solar energetic particle fluences (Lingenfelter and Hudson, 1980; Reedy, 1996).

The distribution in Figure 6 shows a roll-over towards lower event magnitudes, which we attribute to the sensitivity limit for this sample, and the fits below refer

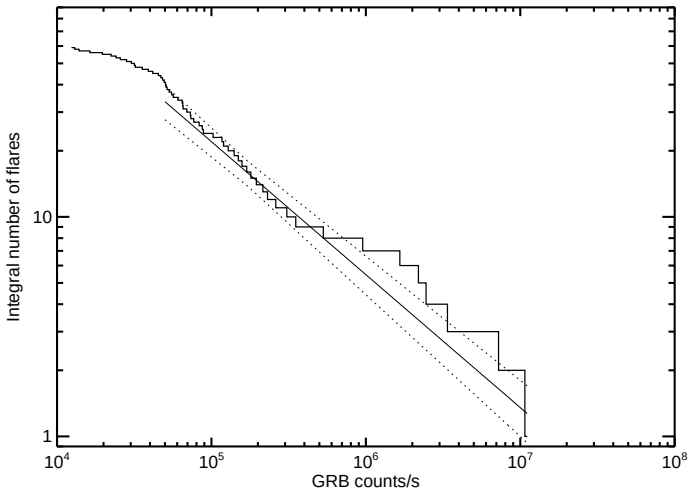

Figure 6. Integral distribution of GRB event magnitudes, selecting events with known GOES occurrence. The solid line shows the best-fit slope of 1.61 ± 0.04 for the differential distribution, and the dotted lines give an approximate range of uncertainties.

to the range above 5×10^4 GRB counts s^{-1} normalized to one AU. This provides a sample of 41 events over the range X2-X25 according to our scaling law. As with previous hard X-ray studies at lower event energies show (see e.g. Crosby *et al.*, 1998), a power-law with an index flatter than -2.0 fits reasonably well. We fit the differential distribution $dN/dS \propto S^{\alpha}$ and use a Monte Carlo method to estimate the error bars directly on the integral distribution shown. This yields α = -1.61±0.04 for the 41 events above the clear knee in the distribution. Note that we have carried out the fit to the integral distribution, which is one power flatter. If we exclude the 9 events with highest GRB counts, including the two most energetic events on the grounds of possible uncertainty regarding the correction factors for GRB saturation, the slope changes to -1.75±0.08. These results are roughly consistent with values obtained for less energetic hard X-ray events (Crosby *et al.* (1998) found 1.58±0.02 from the WATCH experiment). Some studies of soft X-ray events have found steeper slopes (e.g., Veronig *et al.*, 2002) but the slopes may not be directly comparable.

4.5. Loop height estimates

Events located behind the solar limb will be partially occulted, but may nevertheless be visible if the loop height is sufficiently large. The number of GOES X-class flares (with known solar location) was accumulated in ten-degree bins of the angle between *Ulysses* and the flare site. Only events from the complete list in Table 1 for which the GRB instrument registered valid measurements (no contamination of the X-ray detectors by solar particles, and nominal instrument telemetry) have been used.

All but one of the 11 partially occulted flares up to 10° behind the solar limb are visible to the GRB detectors. Between 10° and 20° behind the solar

limb, a third of the 12 flares that occurred are visible. The event of March 24, 2000, is the most extreme example, at an angle of 106.03°. At such an angle the occultation height (the source height, assuming a radial structure) would be 0.041 $R_\odot$ or about 3×10^4 km. This height is consistent with earlier observations made with combined hard X-ray and microwave imaging of flare loops described by Nakajima *et al.* (1985) and Cliver *et al.* (1986).

4.6. A catalog of far-side events

The X-class flares listed in Table 1 that were measured by both GRB and GOES do not constitute an exhaustive record of intense X-ray events throughout the *Ulysses* mission. There are many more signatures in the GRB data that correspond to X-class flares not seen by GOES, implying that the flare sites must be located on the far-side of the Sun from the viewpoint of the Earth.

Table 2 contains a separate list of these flares, providing the date and time of each event, together with the effective GOES X-ray class estimated using the scaling law derived above in Section 4.2. The criteria used to identify these flares were a GRB intensity profile consistent with a solar flare event, a normalized peak count rate greater than a threshold value of 2×10^4 counts s^{-1} and the absence of an X-class flare in the GOES event list. Although it is usually not possible to precisely locate the flare sites for these events, the timing of each GRB event corresponds to a range of potential solar longitudes and latitudes from the known viewing angle of *Ulysses*. Figures showing the GRB response during these inferred far-side events may be found at http://helio.esa.int/ulysses/ftp/public/outgoing/ and in the on-line material.

As expected from the GOES distribution function, the majority of the 116 far-side events thus selected were smaller X-class events. However, there was one inferred X15 event recorded during the intense period of solar activity in 1991. During certain periods of the *Ulysses* orbit, the combination of GRB and GOES measurements provided almost uninterrupted full-Sun coverage of major solar X-ray flare activity.

5. Discussion and conclusions

The *Ulysses* data provide a unique stereoscopic view of solar hard X-ray emission and complement other observations in different ways. In this paper we have summarized the entire data set of energetic (GOES class >X1.0) events to date, a 13-year span that covers the maximum of Carrington cycle 23. This represents only about 10% of the full *Ulysses* GRB solar event list. We present the entire list of X-class flares observed during this time interval after establishing a correlation of the GRB hard X-ray fluxes with the GOES soft X-ray fluxes, which we summarize in the scaling law defined above. This scaling enables us to confirm the magnitude of the November 4, 2003 event as obtained by a simple extrapolation of the saturated GOES light curve at about X25, thus calling into question the somewhat larger fluxes suggested by the ionospheric data. We find the June 1, 1991 event to have had a comparable magnitude despite a deep occultation, and

suggest that it was comparable in magnitude to the November 4, 2003 event, of GOES class X20 or higher.

The *Ulysses* GRB data are consistent with the hypothesis that all GOES X-class flares have hard non-thermal components which extend into the energy range above 25 keV. Our analysis indicates that the 25 keV threshold of the GRB allows some "thermal feedthrough" for the largest events, causing the correlation of GOES magnitude and peak GRB flux to deviate from the near-proportionality found in the RHESSI data. This finding is consistent with the known weak correlation of soft X-ray emission measure and effective temperature, such that more energetic events have larger thermal contributions in the hard X-ray band for a detector with poor spectral resolution. The occurrence frequency distribution continues with the expected flat power law to the greatest events observed (specifically, the two events mentioned above). There is thus no evidence for a cutoff within this sample.

Acknowledgements. KH is grateful for Ulysses support under JPL Contracts 958056 and 1268385. The work of HSH was supported by NASA under grants NAS 5-98033 and NAG5-12878.

Appendix A. *Ulysses* GRB comparison with RHESSI

The *Ulysses* observing time range overlapped with that of RHESSI), which gives us an opportunity for direct photometric comparisons of specific events (e.g., Kane, McTiernan, and Hurley, 2005). We have done a comparison for one well-observed flare, the GOES X8.3 of November 2, 2003. By comparing the corrected counting rates, we confirm a certain level of understanding of these corrections: thermal feed-through, gain (energy scale), pulse pileup, and deadtime, in particular.

Broad-band hard X-ray photometry of solar flares poses particular problems in reconciling the intense thermal component, usually characterized by a maximum kT in the range 1-2 keV, and the much fainter non-thermal tail produced mainly by 10-100 keV electrons. RHESSI partially solves this problem by having a set of shutters (Lin *et al.*, 2002) that control the absorber thickness across the detector. All other solar hard X-ray spectrometers have fixed windows (that of *Ulysses* is 0.3 mm Al in a hemispherical dome configuration). The entrance window serves as a high-pass filter which determines the distribution of pulse heights; in the case of GRB the half-transmission energy thus works out to be about 15 keV, but the steepness of the thermal source spectrum pushes the peak in the pulse-height spectrum to below 10 keV for the lower temperatures. These counts can still contribute to the 25-150 keV observational window, however, via resolution broadening and via pulse pileup (see Appendix 2).

Figure 7 shows the essential elements for a model representation of the pulse-height spectrum produced by a solar thermal source. Note that the peak of the pulse-height distributions fall well below the electronics threshold, and even below the 50% transmission energy of the entrance window. The high-energy tail of these pulse distributions competes with the true hard X-ray spectrum. This causes the morphology smoother light curves seen at lower hard X-ray

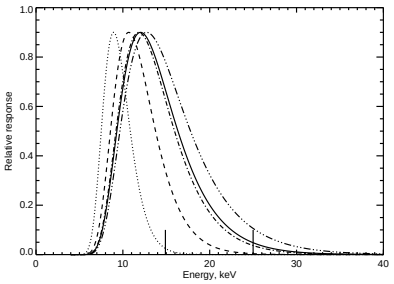

Figure 7. Model pulse height distributions for the *Ulysses*/GRB detector for exponential input spectra with kT = 1, 2, 3, 3.2 , and 4. The solid line (kT = 3.2) shows the spectrum chosen for the pileup studies (Appendix B). The short vertical lines show (left) the minimum 50% transmission energy for GRB, and (right) the electronic channel threshold of 25 keV.

energies, seen not just with *Ulysses*/GRB but with most other scintillator-based spectrometers.

The comparison of counting rates with RHESSI provides essentially complete diagnostics, since RHESSI has high spectral resolution and is not limited to a single telemetry band (25-150 keV) as GRB is. We show the direct comparison in Figure 8, which illustrates a satisfactory comparison early in the event, then a growing divergence later on. The RHESSI live time reached a minimum of about 15% near the time of peak counting rates, and at 25 keV also exhibited the smooth late excess – though not so large – as found in the GRB counts. This behavior can be explained by the poorer spectral resolution of GRB, which is determined by its on-board calibration to be about 48% at 25 keV. There is no need to invoke pulse pileup for this event, and the dead-time corrections for both instruments also seem satisfactory.

Appendix B. The effects of pulse pile-up on the *Ulysses* GRB detector

Pulse pile-up is an effect that occurs at high count rates. Two or more pulses interact in the detector within a time that is too short for the electronics to distinguish them. (Kane and Hudson, 1970; Datlowe, 1975). The resulting signal is a single pulse whose equivalent energy is roughly the sum of the energies of the input pulses. Even if the energies of the input pulses are below the electronics threshold for detection (see Figure 7), the resulting sum signal may be above it. This effect can be an important one when the input spectrum is from a solar flare because of the large fluxes of low-energy photons in the thermal component of the spectrum. These pulses are below the 25 keV counting threshold and so are not counted directly, but if multiple events occur within the detection time window, their sum pulse can exceed the detection threshold. The situation is further complicated by several factors. First, without knowledge of the shape and intensity of the thermal solar X-ray spectrum, a correction cannot be calculated. Second, because the thermal counts are not directly detected, the shape of the input photon spectrum cannot be inferred from the observed

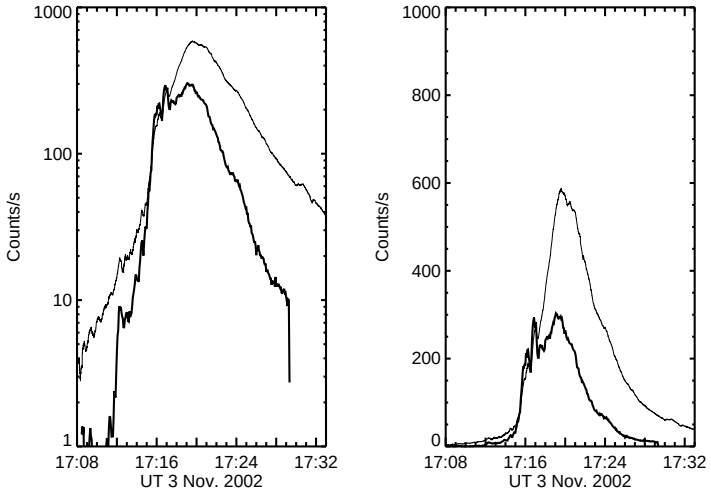

Figure 8. Comparison of RHESSI counting rate (line) with GRB counting rate (dots) for 25-150 keV during the X8.3 flare of November 3, 2003. *Left*, log display; *right*, linear. We attribute the discrepancy after about 17:17 UT to the increasing emission measure of the thermal component directly detected by GRB, rather than via pile-up. During the impulsive phase there is good agreement.

pulse-height spectrum. Note that pulse pile-up is distinct from dead-time effects, since the pulses that pile up do so within a dead-time interval. Both effects can be present at high enough count rates. Also note that thermal feedthrough, described above, depends only on the spectral distribution and should not be confused with rate-dependent effects.

Pile-up can be studied by Monte-Carlo simulations. A very thorough Monte-Carlo program was written for the *Ulysses* detector, and was used to infer the influence of pulse pile-up on the spectra of major flares (Kane *et al.*, 1995). We have now used this program to estimate the effects of pile-up using RHESSI observations for the input spectrum, specifically those described by Holman *et al.* (2003). The thermal component of this flare had an effective temperature of 3.2 keV at maximum. We have simulated the effect that such a spectrum would have on the GRB detector for input counting rates over a wide range, as described below.

The Monte-Carlo program simulates the effects of a parallel beam of X-rays incident on the GRB detector on-axis (as a solar flux would approximately be). Compton and photoelectric K- and L-shell interactions in the hemispherical geometry of the CsI crystals are taken into account, as are Auger electrons, fluorescence, photon scattering out of the crystal, and the escape of scattered electrons. The crystal resolution as a function of energy, and the 0.03 cm thick Al window are also taken into account. For the simulations described here, a bremsstrahlung-like exponential spectrum was used as input between 1 and 150 keV. The input count rate was varied between 10^3 and 10^7 counts s^{-1} with a Poisson interval distribution, and the count rate due to piled-up photons was recorded in the 25-150 keV energy range. If two or three photons interacted in

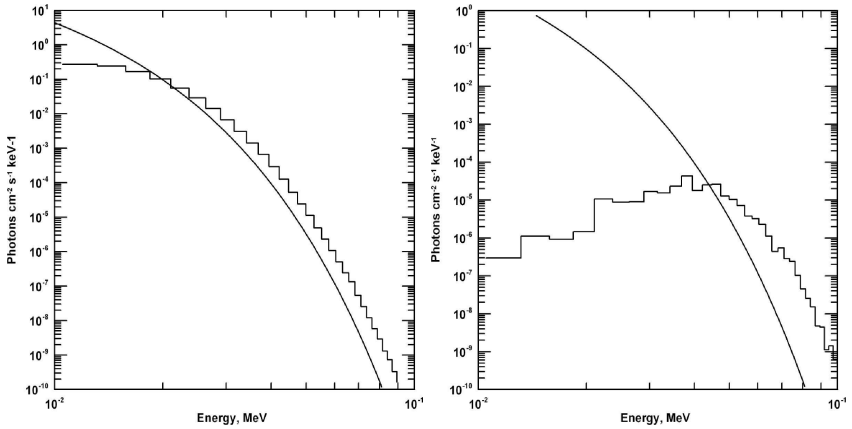

Figure 9.

the detector within a time interval less than one microsecond (the approximate shaping time constant for the GRB detector), they were counted as a single, piled-up count whose energy was the sum of the two energies of the original photons. More than three pile-ups were not tracked, but they will be an important component at very high input count rates. Each simulation used 10^6 input photons.

Figure 9 shows the input and output spectra for 10^3 and 10^7 counts s^{-1}. At 10^3 counts s^{-1}, the output spectrum follows the input spectrum above an energy of about 20 keV. Below this energy, the input spectrum is strongly attenuated due to the Al entrance window (for a parallel input beam, its effective thickness is 0.03 cm only for a single, on-axis point, and increases off-axis due to the hemispherical geometry). At 10^7 counts s^{-1}, the output spectrum is attenuated severely below about 35 keV, due to photons which pile up and are counted at higher energies. The spectrum above 35 keV contains these piled-up counts.

Figure 10 summarize some of these results. The bottom X-axis shows the input count rate at the GRB detector over the 1-150 keV range for a bremsstrahlung-type exponential spectrum with kT = 3.2 keV. This is converted into W m^{-2} at 1 AU in the GOES soft channel along (the upper X-axis), so that the count rates can be compared to GOES fluxes, using the scaling law derived in Section 4.2. The Y-axis shows the piled-up count rate for the GRB experiment in the 25-150 keV range. The piled-up rate is calculated for assumed GRB solar distances of 1 AU and 3.2 AU from the Sun in Figure 10 . The figures show that pile-up is negligible for input count rates up to about 10^5 counts s^{-1}. Even at 10^6 counts s^{-1}, where the average interval between counts is only 1 μs, that is, one pulse-shaping time, the piled-up count rate is small compared to the input count rate. This can be understood as the result of several factors. First, the input count rate is measured over a wider energy range, 1-150 keV, than the piled-up rate (25-150 keV, the GRB passband). Second, for piled-up pulses to actually fall into the GRB passband, they must traverse the entrance window and deposit energies whose sum falls between 25 and 150 keV; many piled-up photons have smaller energies, and would not be counted. Finally, the input

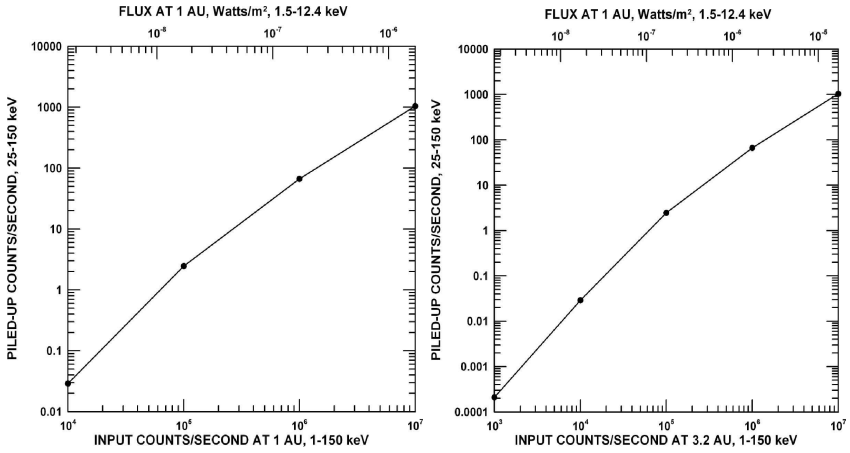

Figure 10.

fluxes are quite small at energies above 20 keV compared to the 1 keV fluxes, due to the shape of the bremsstrahlung spectrum; thus, while they can pile up and fall into the passband, their numbers are very small. We emphasize that two effects have not been treated here. The first is the pile-up of more than three simultaneous pulses. This will become important at input rates above $\sim 3 \times 10^5$ counts s^{-1}, and therefore the piled-up rates in Figure 10 at these input count rates should be considered very conservative lower limits. The second is the pile-up of thermal input photons with non-thermal ones; we have not assumed any non-thermal component in these simulations.

References

Battaglia, M., Grigis, P.C., Benz, A.O.: 2005, Size dependence of solar X-ray flare properties. **439**, 737 – 747. doi:10.1051/0004-6361:20053027.

Brodrick, D., Tingay, S., Wieringa, M.: 2005, X-ray magnitude of the 4 November 2003 solar flare inferred from the ionospheric attenuation of the galactic radio background. *Journal of Geophysical Research (Space Physics)* **110**, 9 – +. doi:10.1029/2004JA010960.

Cliver, E.W., Dennis, B.R., Kiplinger, A.L., Kane, S.R., Neidig, D.F., Sheeley, N.R. Jr., Koomen, M.J.: 1986, Solar gradual hard X-ray bursts and associated phenomena. **305**, 920 – 935. doi:10.1086/164306.

Crosby, N., Vilmer, N., Lund, N., Sunyaev, R.: 1998, Deka-keV X-ray observations of solar bursts with WATCH/GRANAT: frequency distributions of burst parameters. **334**, 299 – 313.

Datlowe, D.W.: 1975, Pulse pile-up in hard X-ray detector systems. *Space Science Instrumentation* **1**, 389 – 406; erratum **2**, 523.

Dennis, B.R.: 1985, Solar hard X-ray bursts. *Solar Phys.* **100**, 465 – 490.

Dennis, B.R.: 1988, Solar flare hard X-ray observations. **118**, 49 – 94.

Dennis, B.R., Zarro, D.M.: 1993, The Neupert effect - What can it tell us about the impulsive and gradual phases of solar flares? **146**, 177 – 190.

Feldman, U.: 1996, Properties of thermal flare plasmas ($3\times10^6 - 3\times10^7 K$) : $observationalresults.Physics\ of\ Plasmas\mathbf{3}, 3203 - -3241$.

Frost, K.J., Dennis, B.R.: 1971, Evidence from Hard X-Rays for Two-Stage Particle Acceleration in a Solar Flare. **165**, 655 – +.

Garcia, H.A.: 1990, Evidence for solar-cycle evolution of north-south flare asymmetry during cycles 20 and 21. **127**, 185 – 197.

Garcia, H.A., McIntosh, P.S.: 1992, High-temperature flares observed in broad-band soft X-rays. **141**, 109 – 126.

Holman, G.D., Sui, L., Schwartz, R.A., Emslie, A.G.: 2003, Electron Bremsstrahlung Hard X-Ray Spectra, Electron Distributions, and Energetics in the 2002 July 23 Solar Flare. **595**, L97 – L101. doi:10.1086/378488.

Hudson, H., Ryan, J.: 1995, High-Energy Particles In Solar Flares. **33**, 239 – 282. doi:10.1146/annurev.aa.33.090195.001323.

Hudson, H.S.: 1978, A purely coronal hard X-ray event. **224**, 235 – 240. doi:10.1086/156370.

Hudson, H.S.: 1991, Solar flares, microflares, nanoflares, and coronal heating. **133**, 357 – 369.

Hurley K.: 1986, Stereoscopic measurements of hard solar X-rays, and related topics. In: Marsden, R.G. (ed.) The Sun and the Heliosphere in Three Dimensions, Astrophysics and Space Science Library, 123, 73 – 86.

Hurley, K., Sommer, M., Atteia, J.L., Boer, M., Cline, T., Cotin, F., Henoux, J.C., Kane, S., Lowes, P., Niel, M.: 1992, The solar X-ray/cosmic gamma-ray burst experiment aboard ULYSSES. **92**, 401 – 410.

Kane S.R., Crannell C.J., Datlowe D., Feldman U., Gabriel A., Hudson H.S., Kundu M.R., Maetzler C., Neidig D., Petrosian V.: 1980, Impulsive phase of solar flares. In: Sturrock, P.A. (ed.) Skylab Solar Workshop II., 187 – 229.

Kane, S.R., Hudson, H.S.: 1970, Re-Interpretation of OSO-III Scintillation Counter Measurements of Hard Solar X-Ray Spectra. **14**, 414 – 418. doi:10.1007/BF00221327.

Kane, S.R., Hurley, K., McTiernan, J.M., Boer, M., Niel, M., Kosugi, T., Yoshimori, M.: 1998, Stereoscopic Observations of Solar Hard X-Ray Flares Made by ULYSSES and YOHKOH. **500**, 1003 – +. doi:10.1086/305738.

Kane, S.R., Hurley, K., McTiernan, J.M., Sommer, M., Boer, M., Niel, M.: 1995, Energy Release and Dissipation during Giant Solar Flares. **446**, L47+. doi:10.1086/187927.

Kane, S.R., McTiernan, J.M., Hurley, K.: 2005, Multispacecraft observations of the hard X-ray emission from the giant solar flare on 2003 November 4. **433**, 1133 – 1138. doi:10.1051/0004-6361:20041875.

Kiplinger A.L., Garcia H.A.: 2004, Soft X-ray Parameters of the Great Flares of Active Region 486. In: Bulletin of the American Astronomical Society, Bulletin of the American Astronomical Society, 36, 739 – +.

Lin, R.P., Dennis, B.R., Hurford, G.J., Smith, D.M., Zehnder, A., Harvey, P.R., Curtis, D.W., Pankow, D., Turin, P., Bester, M., Csillaghy, A., Lewis, M., Madden, N., van Beek, H.F., Appleby, M., Raudorf, T., McTiernan, J., Ramaty, R., Schmahl, E., Schwartz, R., Krucker, S., Abiad, R., Quinn, T., Berg, P., Hashii, M., Sterling, R., Jackson, R., Pratt, R., Campbell, R.D., Malone, D., Landis, D., Barrington-Leigh, C.P., Slassi-Sennou, S., Cork, C., Clark, D., Amato, D., Orwig, L., Boyle, R., Banks, I.S., Shirey, K., Tolbert, A.K., Zarro, D., Snow, F., Thomsen, K., Henneck, R., McHedlishvili, A., Ming, P., Fivian, M., Jordan, J., Wanner, R., Crubb, J., Preble, J., Matranga, M., Benz, A., Hudson, H., Canfield, R.C., Holman, G.D., Crannell, C., Kosugi, T., Emslie, A.G., Vilmer, N., Brown, J.C., Johns-Krull, C., Aschwanden, M., Metcalf, T., Conway, A.: 2002, The Reuven Ramaty High-Energy Solar Spectroscopic Imager (RHESSI). **210**, 3 – 32. doi:10.1023/A:1022428818870.

Lin, R.P., Schwartz, R.A., Pelling, R.M., Hurley, K.C.: 1981, A new component of hard X-rays in solar flares. **251**, L109 – L114. doi:10.1086/183704.

Lingenfelter R.E., Hudson H.S.: 1980, Solar particle fluxes and the ancient sun. In: Pepin, R.O., Eddy, J.A., Merrill, R.B. (eds.) The Ancient Sun: Fossil Record in the Earth, Moon and Meteorites., 69 – 79.

Nakajima, H., Dennis, B.R., Hoyng, P., Nelson, G., Kosugi, T., Kai, K.: 1985, Microwave and X-ray observations of delayed brightenings at sites remote from the primary flare locations. **288**, 806 – 819. doi:10.1086/162851.

Neupert, W.M.: 1968, Comparison of Solar X-Ray Line Emission with Microwave Emission during Flares. *ApJ* **153**, L59 – +.

Orwig, L.E., Frost, K.J., Dennis, B.R.: 1980, The hard X-ray burst spectrometer on the Solar Maximum Mission. **65**, 25 – 37.

Osten, R.A., Drake, S., Tueller, J., Cummings, J., Perri, M., Moretti, A., Covino, S.: 2007, Nonthermal Hard X-Ray Emission and Iron Kα Emission from a Superflare on II Pegasi. **654**, 1052 – 1067. doi:10.1086/509252.

Reedy R.C.: 1996, Constraints on Solar Particle Events from Comparisons of Recent Events and Million-Year Averages. In: Balasubramaniam, K.S., Keil, S.L., Smartt, R.N. (eds.) Solar Drivers of the Interplanetary and Terrestrial Disturbances, Astronomical Society of the Pacific Conference Series, 95, 429 – +.

Reedy R.C., Marti K.: 1991, Solar-cosmic-ray fluxes during the last ten million years. In: Sonett, C.P., Giampapa, M.S., Matthews, M.S. (eds.) The Sun in Time., 260 – 287.

Smith H.J., Smith E.V.P.: 1963, Solar flares. New York, Macmillan [1963].

Thomson, N.R., Rodger, C.J., Dowden, R.L.: 2004, Ionosphere gives size of greatest solar flare. **31**, 6803 – +. doi:10.1029/2003GL019345.

Tomczak, M.: 2001, The analysis of hard X-ray radiation of flares with occulted footpoints. **366**, 294 – 305. doi:10.1051/0004-6361:20000204.

Veronig, A., Temmer, M., Hanslmeier, A., Otruba, W., Messerotti, M.: 2002, Temporal aspects and frequency distributions of solar soft X-ray flares. **382**, 1070 – 1080. doi:10.1051/0004-6361:20011694.